Polypyrrole–vanadium oxide nanocomposite: polymer dominates crystallanity and oxide dominates conductivity

Swarup Roy[1] · Suryakant Mishra[1] · Priyanka Yogi[1] · Shailendra K. Saxena[1,2] · Vikash Mishra[1] · Pankaj R. Sagdeo[1] · Rajesh Kumar[1]

Abstract

A hybrid nanocomposite of polypyrrole (Ppy)–V_2O_5 has been fabricated and characterized for better understanding of material enabling one to use this for appropriate application as the nanocomposite shows better thermal stability. The characterization has been done using XRD, FT-IR, FESEM, and UV–Vis for their structure, surface morphology, respectively, along with TGA and two-probe method used for checking thermal stability, and DC electrical conductance and dielectric behavior of the electrical phenomena of sample. The analysis of XRD demonstrates that crystallinity of nanocomposites is the same as that of the polymer, even though interaction between conducting Ppy and V_2O_5 is present as evident from FT-IR spectroscopy. A variation in bandgap, in comparison with Ppy, is observed when V_2O_5 is added into it. The microstructural study of nanocomposites shows encapsulation of V_2O_5 particles in Ppy matrix with changes in morphology with increase in doping. Conductance results show that electrical conductivity of Ppy decayed on adding V_2O_5. It has also been found that addition of V_2O_5 in Ppy has noticeable effect on the dielectric properties.

1 Introduction

Organic–inorganic nanocomposites have been identified as new class of materials due to their improved properties compared to pure bulk conducting polymers or inorganic materials [1, 2]. Conducting polymers have drawn interest because of their diverse structures, special doping mechanism, excellent environmental stability, good solution process ability, and high conductivity [3]. The main attractions of conducting polymer composites are their potential applications in batteries [4], electrochemical display devices [5], molecular electronics [6], electrical-magnetic shields, microwave-absorbing materials [7], etc. Furthermore, conducting polymers also exhibit a wide range of electrical, optical, and magnetic properties. Amongst various such polymers, Ppy has high electrical conductivity and substantial air stability, and this has been effectively used in the preparation of different nanocomposites [8, 9]. Ppy has attracted pronounced attention due to its unique electrical conductivity, optical property, redox property, efficient electron donors and good transporters of electron, and high mobility of charge carriers [10–14].

On the other hand, vanadium oxide (V_2O_5), a transition metal oxide, has a layered structure and exhibits good electrochemical activity. The V_2O_5 shows novel characteristics including electrochromism [15]. In rechargeable lithium batteries, the charge storage behavior of deposits of hydrated V_2O_5 is used [16]. The layered structure and redox ability of V_2O_5 allow the addition of a number of foreign species like polymers and which lead to the grounds of hybrid materials with a mixed valence of vanadium (V^{4+}/V^{5+}) [17]. Organic–inorganic hybrid structures have been planned to achieve new materials with better properties due to the synergic effects of the monomer [18]. The intercalation of conducted polymers into layered inorganic hosts has drawn great attention and is a topic of research interest. To improve the electrochemical properties of V_2O_5, its hybrid with conducted polymers has been studied in recent years [19, 20]. According to the importance of organic–inorganic

✉ Rajesh Kumar
rajeshkumar@iiti.ac.in

1 Material Research Laboratory, Discipline of Physics, Indian Institute of Technology Indore, Simrol 453552, India

2 Present Address: National Institute for Nanotechnology, University of Alberta, Alberta, Canada

hybrid composite material, it will be worth to understand Ppy–V_2O_5 nanocomposites' synthesis and characterization along with optical and electrical properties.

The aim of this present study is to report a facile oxidative chemical polymerization synthesis and characterization of Ppy–V_2O_5 nanocomposite. The structural and morphological study of Ppy–V_2O_5 nanocomposites has been investigated here. Electrical and optical properties of synthesized nanocomposite have also been studied. The present study is expected to provide more insight on the optical and electrical properties of the Ppy–V_2O_5 nanocomposite.

2 Materials and methods

Pyrrole and ammonium persulphate (APS) have been purchased from Sigma chemicals and used as received. All other chemicals are of analytical grade and used without further purification. Polymerization of pyrrole monomer has carried out in chemical oxidative environment. For the preparation of Ppy, 50 ml of 0.2 M aqueous pyrrole added drop wise to 50 ml of 0.2 M aqueous solution of APS under constant magnetic stirring for 2 h at 5–10 °C. The resulting black precipitates so obtained was then filtered and washed with copious amount of distilled water followed by ethanol until the filtrate became colorless. Ppy so obtained then dried by keeping in oven at 70 °C for overnight. Dry powdered sample was then made into pellets using a stainless steel die of 1.3 cm diameter in a hydraulic press under a pressure of 5 tons.

To prepare Ppy–V_2O_5 composites, different weight percent, 10, 20, and 40 wt% of V_2O_5 were mixed with pyrrole. The mixtures are stirred with magnetic stirrers in ice water baths for 30 min to get a uniform suspension of the composite. The work-up procedure is the same as described above. The details of sample are given in Table 1.

The FT-IR spectrum has been recorded on a Perkin-Elmer-Spectrum spectrophotometer in the range of 500–4500 cm^{-1}. The samples have been prepared in the pellet form using a spectroscopic grade KBr powder. Morphological studies have been carried out with the help of a SUPRA S50 field emission scanning electron microscope (FESEM). The X-ray diffraction measurements have been performed using Bruker-AXS Model X-ray diffractometer.

Table 1 Details of Ppy–V_2O_5 composites sample

Sample name	Doping percentage of V_2O_5
Ppy	Polypyrrole only
Ppyv1	Polypyrrole + 10 wt% of V_2O_5
Ppyv2	Polypyrrole + 20 wt% of V_2O_5
Ppyv3	Polypyrrole + 40 wt% of V_2O_5

Thermogram of the polymer sample has been recorded using Mettler-Toledo 851 thermogravimetric analyzer in the presence of N_2 atmosphere from room temperature to 1000 °C at a heating rate of 10 °C/min. UV–Vis spectra have been measured in Agilent Carry 60 UV–Vis spectrophotometer. Electrical resistance measurements have been carried out by the two-probe technique. A Keithley make two-probe setup (236) has been used to provide the necessary voltage and measure the resulting currents. Two wires have been used instead of the two probes, and they are connected to the pellet of synthesized materials using silver paint and circled stickers with a known surface area. Dielectric properties have been investigated by an LCR meter (6500B, WAYNE KERR at the frequency of 10^2–10^6 Hz at room temperature).

3 Results and discussion

Figure 1 represents the FT-IR spectra of pure Ppy and Ppy–V_2O_5 composite materials as listed in Table 1. The peaks attributed to C–H wagging [21] appear at 920 cm^{-1}. The spectrum of bulk Ppy shown in Fig. 1 confirmed the formation of Ppy as a result of polymerization.

The band at 1552 cm^{-1} and a weak band at 1473 cm^{-1} are assigned to stretching vibration of C=C and C–C, respectively, in the pyrrole ring. When FT-IR spectra of Ppy composites with varying weight percentages of V_2O_5 were compared with the pure Ppy, it was observed that major characteristic peaks of Ppy were present with a slight shift in some of the frequencies. The bands at 1187 and 920 cm^{-1} indicate the doping state of Ppy, whereas peak at 790 cm^{-1} signifies that the pyrrole is being polymerized. The peak at 1048 cm^{-1} can be assigned to the C–H deformation of Ppy. There is also a presence of small band at 1700 cm^{-1} corresponding to V–O–C stretching mode in each case. The peaks observed in the present work match well with
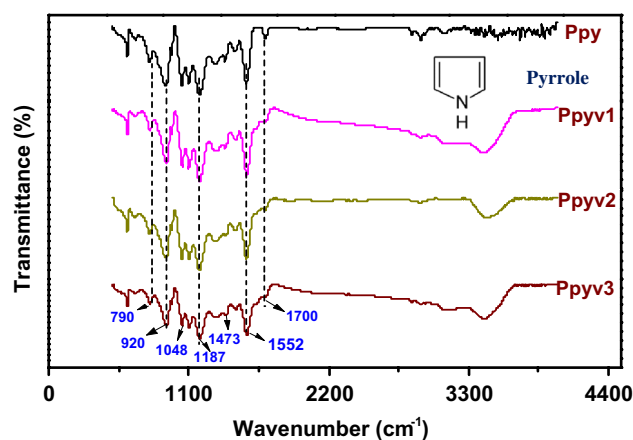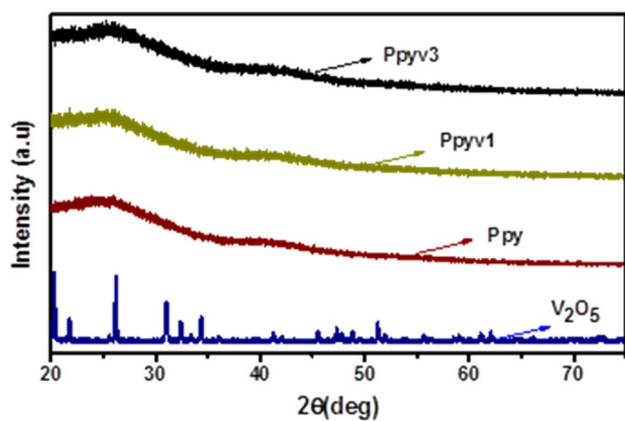

Fig. 1 FT-IR spectra of Ppy–V_2O_5 composite

Fig. 2 XRD patterns of Ppy–V_2O_5 nanocomposite

Fig. 3 Thermogram of Ppy–V_2O_5 nanocomposite

the ones available in the literature confirming the formation of Ppy [22]. Significant changes are observed in the position and shape of the stretching vibration peaks of the Ppy–V_2O_5 composites framework compared with Ppy [23]. Resulting insight suggests that there is a possible formation of Ppy–V_2O_5 composite phase, and for better understanding and characterization, XRD study has been carried out in the next section.

Figure 2 shows the XRD patterns of Ppy and Ppy–V_2O_5 composites which shows that Ppy powder is amorphous in nature. All XRD patterns have broad peaks at $2\theta = 22°$–$25°$ indicating diffraction hallows corresponding to amorphous phase with no clear indication of crystallinity [24, 25]. This broadening of peaks can be ascribed to the scattering of the bare Ppy chains at the interplanar spacing. This indicates that the intercalated product is present with low crystallinity ascribed to the short-range order [20, 26]. To get more details about the synthesized Ppy–V_2O_5 composites materials, TGA study has been performed in the next section.

The thermal behavior of the as-prepared composite samples has been studied using TGA in N_2 atmosphere and presented in Fig. 3. The careful observation of the thermogram of Ppyv2 shows a weight loss of 15% up to 200 °C which can be attributed to the release of moisture/water adsorbed on the sample [27]. The smooth weight loss from 200 to 500 °C is mainly contributed by the elimination of strongly bound water, impurities, and unreacted monomers of composite. While the continuous and rapid weight loss from 500 °C onwards is due to the degradation and decomposition of Ppy–V_2O_5. Thus, the Ppy–V_2O_5 composite may be considered as thermally more stable compared to pure Ppy which might be related to the combination of V_2O_5 and Ppy. The more the amount of V_2O_5 present within the composite, there may be stronger bond formation with the Ppy which does not allow easy degradation and in turn shows greater thermal stability. For details, morphological characterization using FESEM study was carried out in the following section.
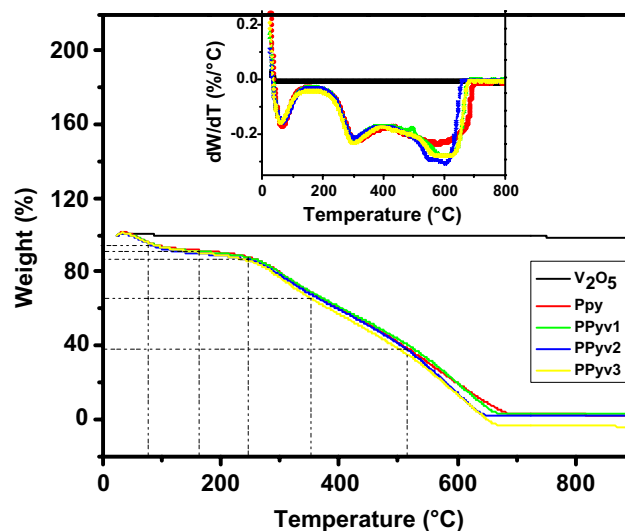
FESEM micrographs of Ppy and Ppy–V_2O_5 composites are shown in Fig. 4a–d. Figure 4b–d suggests possibility of encapsulation of V_2O_5 in Ppy matrix along with grain agglomeration with varying morphology on increasing doping in samples Ppyv1, Ppyv2, and Ppyv3. Synthesized Ppy particles are roughly spherical in shape and in the size range of 100–200 nm (Fig. 4a) which decreases with increase in doping with consistent agglomeration in all the samples (Fig. 4b, c). Successful synthesis of Ppy–V_2O_5 nanocomposites is evident from SEM micrographs in Fig. 4. For better understanding of optical phenomenon of synthesized nanocomposite materials, we have carried out spectroscopic studies.

Figure 5 shows UV–Vis spectra of Ppy along with the composites showing absorption peak at 446 nm (2.77 eV) as reported in the literature [28]. The absorption spectrum exhibits this absorption at ~ 450 nm which is characteristic of π–π* transition of neutral Ppy. The nanocomposites of Ppy–V_2O_5 also have consistent peak at ~ 440 nm (slight blue shift in peak observed due to the composite formation) mainly of neutral Ppy. Resulting insight suggests that there may be structural changes upon increase in dopant percentage of V_2O_5 in Ppy. The blue shift indicates a decrease in the effective conjugation of the Ppy, which may change the secondary structure of Ppy. The energy bandgap of the synthesized nanocomposite has been calculated [29] and the details presented in supplementary information (SI) (Fig. S1). To understand the electrical properties of synthesized nanocomposite materials, following study has been carried out.

An Ohmic behavior is observed in *I–V* characteristic plots for each composite when measured at room temperature, as shown in Fig. 6. The appreciable linear increase in DC

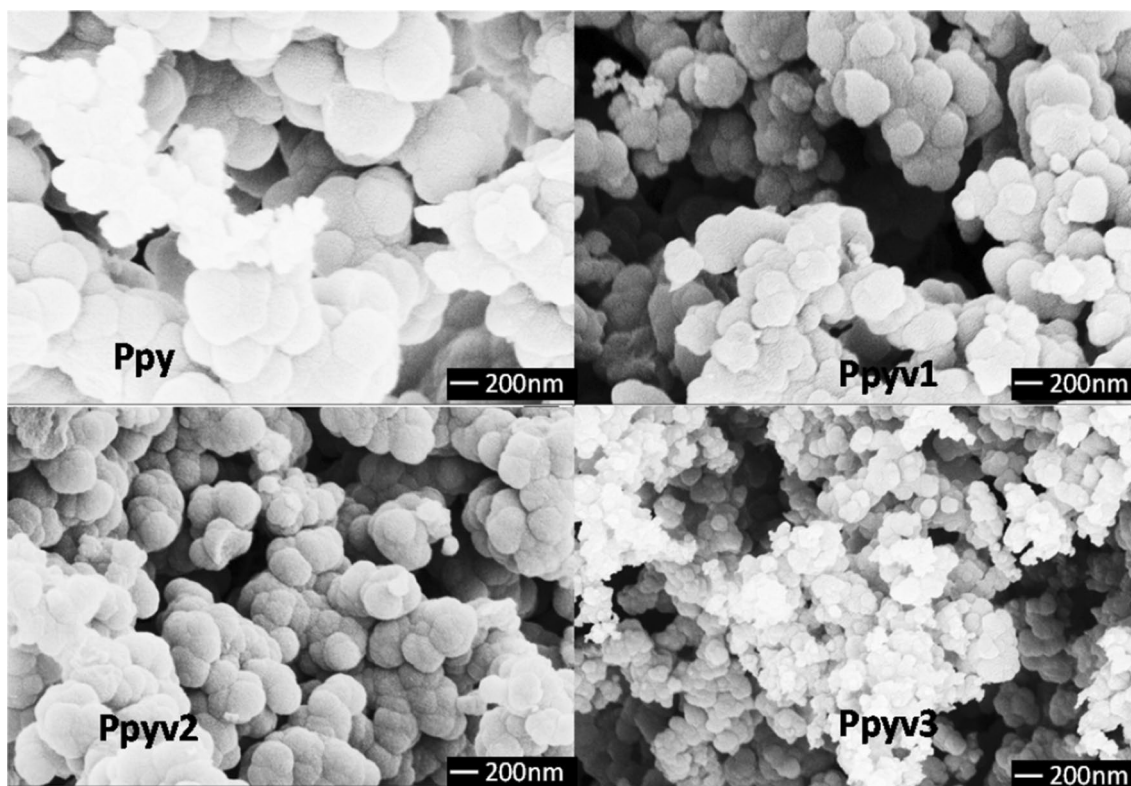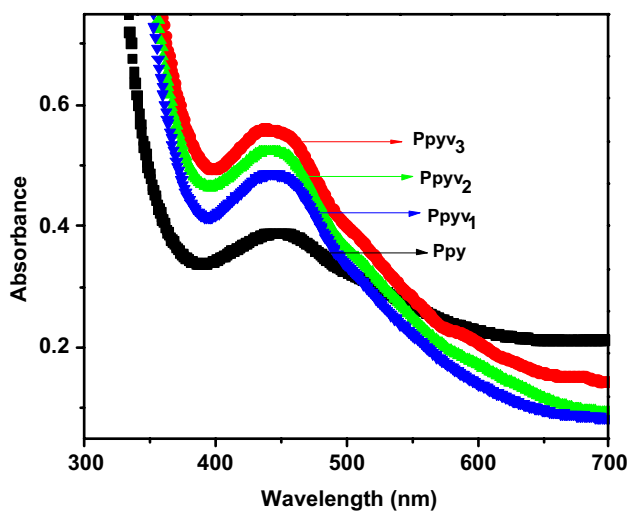**Fig. 4** FESEM micrographs of Ppy–V_2O_5 nanocomposite

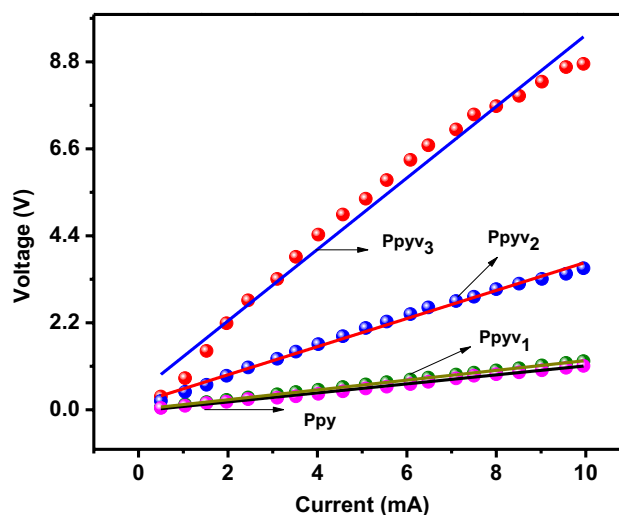**Fig. 5** UV–Vis spectra of Ppy–V_2O_5 nanocomposite

Fig. 6 *I–V* characteristics plots of Ppy–V_2O_5 nanocomposites

conductivity may be due to detraction in the mobility of electrons owing to highly extended chain conformation to increase tunneling probability in all synthesized composites and is due to the versatile semiconducting nature of V_2O_5 [30, 31] which is contrary to some previous reported work in which dopant material was an insulator [32, 33]. It

was observed that the electrical resistance increases with increase in dopant concentration, and hence, conductivity decreases (Fig. S2 in supporting information).

Low DC conductivity of pure Ppy is due to the random orientation of its particles, poor link among the polymer chains through the grain boundaries and compactness.

Electrical conductivity of Ppy is 144.07 S cm^{-1}, while in Ppyv1, Ppyv2, and Ppyv3 nanocomposite, electrical conductivity is 133.47, 46.54, and 37.91 S cm^{-1} respectively. Results show that electrical conductivity of Ppy decayed on adding V_2O_5. In case of Ppy–Fe_2O_3 composite [34], it has been observed that the Ppy conductivity initially increases from 6.00 to 34.00 S cm^{-1} and then reduced to 9.92 S cm^{-1}. Whereas in case of Ppy–ZnO composite [35], it has been describes that increase of conductivity from 6 to 18.52 S cm^{-1} with the increase in ZnO content at Ppy. In general, the conductivity of composite depends on the characteristics of the composite like shape, particle size, surface area, crystallinity, and morphology. The decrease of conductivity of Ppy–V_2O_5 nanocomposites may be ascribed to the behavior of V_2O_5 in the nanocomposites or may be due to increasing amount of V_2O_5, the possibility of bond formation between Ppy on the surface of V_2O_5 is increased, and the relative contents of the conducting Ppy decreased [36]. From the SEM, it is observed that agglomeration and decrease in size of particles occur with increasing addition of V_2O_5. Therefore, decrease in conductivity may be due to the agglomeration of nanocomposite which leads to obstacle in the movement of charge through the composite which, in turn, lower conductivity in the presence of higher dopant.

Dependence of dielectric constant as a function of frequency ranging from 10^2 to 10^6 Hz at room temperature for the pure Ppy and its composites is plotted in Fig. 7. It is observed that the values of dielectric constant decrease with increasing amount of V_2O_5 at increasing frequency from 10^2 to 10^6 Hz. The decrease of dielectric constant with increasing frequency is an expected behavior in most dielectric materials, but the difference between the values at low and high frequencies is significant in the case of conductive polymers [37, 38].
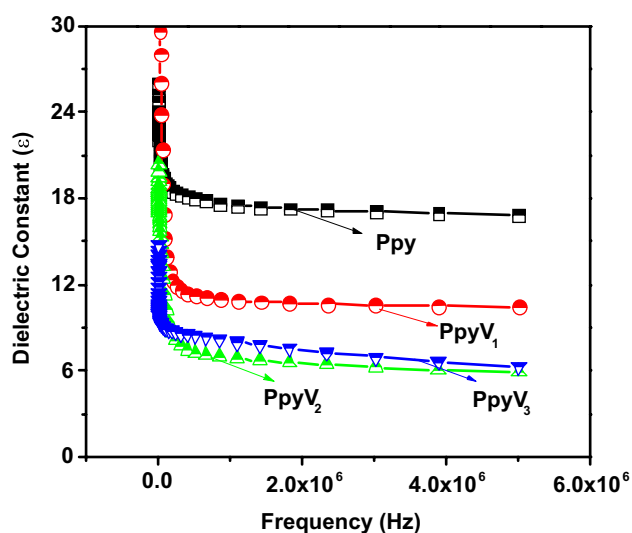
The high values of dielectric constant at low frequencies are due to interfacial polarization, i.e., the building up of bound charges at interfaces within the bulk samples. Dielectric constant decreases as the frequency is increasing and this remains nearly unaltered after the frequency of 10^5 Hz. The decrease in dielectric constant with increasing frequency may arise either from the lag of dipole oscillations behind those of the applied AC electrical field at high frequencies or due to the need of more thermal energy to disturb the ordered dipoles at higher frequencies of the applied field. The dielectric constant for the composites reduced with higher content of V_2O_5 (10, 20, and 40%) which implies that increase in dopant content, there is a decrease of the dielectric constant.

4 Conclusion

In summary, the study of Ppy–V_2O_5 nanocomposites, with spherical shape and granular morphology, shows that crystallinity is mainly dominated by Ppy. A slight variation in the bandgap is observed in the composite in comparison with the Ppy. The Ppy–V_2O_5 nanocomposites show better thermal stability as compared to Ppy. The conductivity of nanocomposites is lesser that that of Ppy due to the effect of V_2O_5, an insulating material. It is also found that the dielectric constant of the nanocomposites decreased with increasing frequency for a given doping concentration and the same also decreases with increasing dopant content for a given frequency. The present results established that by embedding V_2O_5 in Ppy polymer matrix, the optical and electrical properties of the nanocomposites can be tuned.

Fig. 7 Dielectric constant versus frequency plot for Ppy–V_2O_5 nanocomposites

References

1. R. Gangopadhyay, A. De, Chem. Mater. **12**, 608 (2000)
2. T.J. Rivers, T.W. Hudson, C.E. Schmidt, Adv. Funct. Mater. **12**, 33 (2002)
3. N.K. Guimard, N. Gomez, C.E. Schmidt, Prog. Polym. Sci. **32**, 876 (2007)
4. H. Nguyen-Cong, V. de la Garza Guadarrama, J.L. Gautier, P. Chartier, Electrochim. Acta. **48**, 2389 (2003)
5. R. Gangopadhyay, A. De, Eur. Polym. J. **35**, 1985 (1999)
6. M.-K. Song, Y.-T. Kim, B.-S. Kim, J. Kim, K. Char, H.-W. Rhee, Synth. Met. **141**, 315 (2004)
7. D.A. Makeiff, T. Huber, Synth. Met. **156**, 497 (2006)
8. A. Bhattacharya, D.C. Mukherjee, J.M. Gohil, Y. Kumar, S. Kundu, Desalination **225**, 366 (2008)

9. Q. Gao, Y. Wang, D. He, C. Ju, L. Gao, M. Fu, J. Nanosci. Nanotechnol. **11**, 9836 (2011)
10. H. Liang, X. Li, Appl. Catal. B Environ. **86**, 8 (2009)
11. G. Chakraborty, K. Gupta, A.K. Meikap, R. Babu, W.J. Blau, Solid State Commun. **152**, 13 (2012)
12. F. Huguenin, R.M. Torresi, J. Phys. Chem. C **112**, 2202 (2008)
13. C.A. Ferreira, S.C. Domenech, P.C. Lacaze, J. Appl. Electrochem. **31**, 49 (2001)
14. F. Han, D. Li, W.-C. Li, C. Lei, Q. Sun, A.-H. Lu, Adv. Funct. Mater. **23**, 1692 (2013)
15. S. Mishra, H. Pandey, P. Yogi, S.K. Saxena, S. Roy, P.R. Sagdeo, R. Kumar, Opt. Mater. **66**, 65 (2017)
16. A.-M. Cao, J.-S. Hu, H.-P. Liang, L.-J. Wan, Angew. Chem. Int. Ed Engl. **44**, 4391 (2005)
17. T. Chirayil, P.Y. Zavalij, M.S. Whittingham, Chem. Mater. **10**, 2629 (1998)
18. A. Sellinger, P.M. Weiss, A. Nguyen, Y. Lu, R.A. Assink, W. Gong, C.J. Brinker, Nature **394**, 256 (1998)
19. F. Huguenin, E.M. Girotto, R.M. Torresi, D.A. Buttry, J. Electroanal. Chem. **536**, 37 (2002)
20. C. Piewnuan, J. Wootthikanokkhan, P. Ngaotrakanwiwat, V. Meeyoo, S. Chiarakorn, Superlattices Microstruct. **75**, 105 (2014)
21. H.J. Kharat, K.P. Kakde, P.A. Savale, K. Datta, P. Ghosh, M.D. Shirsat, Polym. Adv. Technol. **18**, 397 (2007)
22. K. Arora, A. Chaubey, R. Singhal, R.P. Singh, M.K. Pandey, S.B. Samanta, B.D. Malhotra, S. Chand, Biosens. Bioelectron. **21**, 1777 (2006)
23. C. Zhang, Q. Li, J. Li, Synth. Met. **160**, 1699 (2010)
24. R. Partch, S.G. Gangolli, E. Matijević, W. Cal, S. Arajs, J. Colloid Interface Sci. **144**, 27 (1991)
25. J. Ouyang, Y. Li, Polymer **38**, 3997 (1997)
26. S. Ebrahimiasl, A. Zakaria, A. Kassim, S.N. Basri, Int. J. Nanomed. **10**, 217 (2014)
27. B. Li, Y. Xu, G. Rong, M. Jing, Y. Xie, Nanotechnology **17**, 2560 (2006)
28. H. Shiigi, M. Kishimoto, H. Yakabe, B. Deore, T. Nagaoka, Anal. Sci. **18**, 41 (2002)
29. A.R. Sadrolhosseini, S. Abdul Rashid, A.S.M. Noor, A. Kharazmi, H.N. Lim, M.A. Mahdi, J. Nanomater. **2016**, e1949042 (2016)
30. L. Geng, Y. Zhao, X. Huang, S. Wang, S. Zhang, W. Huang, S. Wu, Synth. Met. **156**, 1078 (2006)
31. K. Gupta, P.C. Jana, A.K. Meikap, Synth. Met. **160**, 1566 (2010)
32. P. Mavinakuli, S. Wei, Q. Wang, A.B. Karki, S. Dhage, Z. Wang, D.P. Young, Z. Guo, J. Phys. Chem. C **114**, 3874 (2010)
33. Z. Guo, K. Shin, A.B. Karki, D.P. Young, R.B. Kaner, H.T. Hahn, J. Nanoparticle Res **11**, 1441 (2009)
34. F. Kanwal, S.A. Siddiqi, A. Batool, M. Imran, W. Mushtaq, T. Jamil, Synth. Met. **161**, 335 (2011)
35. A. Batool, F. Kanwal, M. Imran, T. Jamil, S.A. Siddiqi, Synth. Met. **161**, 2753 (2012)
36. J.-C. Xu, W.-M. Liu, H.-L. Li, Mater. Sci. Eng. C **25**, 444 (2005)
37. I. Haldar, A. Nayak, J. Nanosci. Nanotechnol. **17**, 4658 (2017)
38. K. Ahmed, F. Kanwal, S.M. Ramay, A. Mahmood, S. Atiq, Y.S. Al-Zaghayer, Adv. Condens. Matter Phys. **2016**, e4793434 (2016)